Using metal precursors to passivate oxides for area selective deposition

Cite as: J. Vac. Sci. Technol. A 41, 033407 (2023); doi: 10.1116/6.0002413 Submitted: 9 December 2022 · Accepted: 27 March 2023 ·







Published Online: 25 April 2023







AFFILIATIONS

Department of Materials Science and Engineering, University of Illinois at Urbana-Champaign, 1304 W. Green St. MC 246, Urbana, Illinois 61801

Note: This paper is a part of the Special Topic Collection on Area Selective Deposition.

a)Electronic mail: abelson@illinois.edu

ABSTRACT

Although it has long been known that metal-containing compounds can serve as catalysts for chemical vapor deposition (CVD) of films from other precursors, we show that metal-containing compounds can also inhibit CVD nucleation or growth. For two precursors A and B with growth onset temperatures $T_{\rm gA} < T_{\rm gB}$ when used independently, it is possible that B can inhibit growth from A when the two precursors are coflowed onto a substrate at a temperature (T) where $T_{\rm gA} < T < T_{\rm gB}$. Here, we consider three precursors: AlH₃·NMe₃ ($T_{\rm g} = 130\,^{\circ}$ C, $T_{\rm gB} = 130\,^{\circ}$ C, $T_{\rm gB} = 130\,^{\circ}$ C, and AlMe₃ ($T_{\rm g} = 300\,^{\circ}$ C). We find that (i) nucleation of Al from AlH₃·NMe₃ is inhibited by Hf(BH₄)₄ at 150 °C on two oxide surfaces (Si with native oxide and borosilicate glass), (ii) nucleation and growth of HfB₂ is inhibited by AlMe₃ at 250 °C on native oxide substrates and on HfB₂ nuclei, and (iii) nucleation of Al from AlH₃·NMe₃ is inhibited by AlMe₃ at 200 °C on native with growth onset temperatures $T_{\rm gA} < T_{\rm gB}$ when used independently, it is possible that B can inhibit growth from A when the two precursors 250 °C on native oxide substrates and on HfB2 nuclei, and (iii) nucleation of Al from AlH3·NMe3 is inhibited by AlMe3 at 200 °C on native oxide substrates. Inhibition by Hf(BH₄)₄ is transient and persists only as long as its coflow is maintained; in contrast, AlMe₃ inhibition of HB, growth is more permanent and continues after coflow is halted. As a result of nucleation inhibition, AlMe, coflow enhances selectivity. HfB₂ growth is more permanent and continues after coflow is halted. As a result of nucleation inhibition, AlMe₃ coflow enhances selectivity for HfB₂ deposition on Au (growth) over Al₂O₃ (nongrowth) surfaces, and Hf(BH₄)₄ coflow makes it possible to deposit Al on Al nuclei and not on the surrounding oxide substrate. We propose the following criteria to identify candidate molecules for other precursor-inhibitor combinations: (i) the potential inhibitor should have a higher T_g than the desired film precursor, (ii) the potential inhibitor should be unreactive toward the desired film precursor, and (iii) at the desired growth temperature, the potential inhibitor should adsorb strongly enough to form a saturated monolayer on the intended nongrowth surface at accessible inhibitor pressures.

Published under an exclusive license by the AVS. https://doi.org/10.1116/6.0002413 HfB2 growth is more permanent and continues after coflow is halted. As a result of nucleation inhibition, AlMe3 coflow enhances selectivity

I. INTRODUCTION

The fabrication of modern integrated devices depends on the ability to create precise patterns of metals and other materials with feature sizes on the nanometer length scale. Even when the patterning is successful, however, slight misalignments with respect to underlying features can render the device inoperable. One way to avoid the need for precise alignment uses area selective deposition (ASD), in which films grow only on certain surfaces on a patterned substrate, such as on metals but not on oxides. This approach depends on there being a large difference in nucleation and growth rates on the intended growth and nongrowth surfaces. ASD can be carried out in atomic layer deposition (ALD), chemical vapor deposition (CVD), and even some physical vapor deposition techniques. 1-5 Here, we focus on ASD processes in thermal CVD; we note that all precursors used here may also be used in ALD.6,

Selective CVD on one surface over another can sometimes be enhanced by introducing an inhibitor that suppresses nucleation or growth. The inhibitor can be introduced either as a single dose before film growth or by continuous dosing (coflow) during growth. For example, self-assembled monolayers (SAMs) can serve as single-dose CVD inhibitors that work by blocking surface reactive sites and preventing precursor transport through the SAM to the surface.⁸⁻¹¹ Small molecules can also serve as single-dose inhibitors if they bind irreversibly to the surface, but, if they bind reversibly, they must be supplied continuously. Some examples of small molecules that have been used as inhibitors of CVD growth are β-diketonates, ^{12–14} ammonia, ^{15,16} and alkoxy- or aminosilanes. ^{17–19}

²Department of Chemistry, University of Illinois at Urbana-Champaign, 505 S Mathews Ave., Urbana, Illinois 61801



Most of these inhibitors act by blocking surface reactive sites. For small molecule inhibitors, the inhibition effect is lost if the surface is heated to a temperature at which the inhibitor either reacts or desorbs too quickly to maintain a high surface coverage.

Metal-containing molecules have occasionally been used in exactly the opposite way, i.e., as catalysts for the nucleation and growth of thin films. For example, it is well known that CVD of many metal-containing phases shows an autocatalytic growth behavior.^{20–22} In addition, pretreatment of surfaces with TiCl₄ is known to accelerate nucleation of aluminum CVD and lead to smoother films, 23-25 and metal dimethylamido precursors can promote nucleation of Al, Co, and HfB2.

Here, we show that metal-containing compounds can also inhibit CVD nucleation or growth, and this work adds to an emerging field of these new candidate inhibitors.²⁷ For a given growth time, this inhibition occurs in a temperature window above the onset temperature (Tg) at which the intended growth precursor will nucleate and grow a film, but below the onset temperature at which the inhibitor (here, the metal-containing compound) will nucleate and grow. We demonstrate this behavior in three systems: the nucleation of aluminum from trimethylamine alane, AlH₃·NMe₃ (TMAA),²⁴ being inhibited by hafnium borohydride Hf(BH₄)₄ (Refs. 29 and 30) and also by trimethylaluminum AlMe3,31 and the nucleation and growth of HfB₂ from Hf(BH₄)₄ being inhibited by AlMe₃.³¹ Similar behavior can be expected for other metal-containing compounds under appropriate circumstances.

II. EXPERIMENT

The single-source HfB2 precursor, Hf(BH4)4, was prepared by a literature route. ^{29,32,33} The aluminum precursors trimethylamine alane (TMAA)^{23,28} and trimethylaluminum (AlMe₃)³¹ were purchased (Gelest) and used as received. All three precursors have room temperature vapor pressures—Hf(BH₄)₄ (15 Torr), TMAA (1.2 Torr), and AlMe₃ (11 Torr)—that are high enough that no precursor heating or carrier gas is needed.

Several substrates were employed. Si wafers were degreased by sequential rinsing with acetone, isopropanol, and water. Trench substrates obtained from Novellus were made of patterned SiN_x on a Si wafer support. Dry N2 was blown over the trench substrates to clean off particles; liquid solvents were not used due to poor infiltration and escape of liquids from the trenches. For selective growth experiments with AlMe3 as an inhibitor, some silicon substrates were coated with 100 cycles of ALD Al₂O₃ on top of a thin TiO₂ layer, and other silicon substrates were coated with 150 nm Au on top of a thin Cr adhesion layer. These substrates were degreased with acetone-isopropanol-water and dried before being loaded simultaneously into the chamber (one Al₂O₃ and one Au substrate per experiment).

Flow CVD experiments were performed in a cold-wall, turbopumped CVD system having a base pressure of 4×10^{-7} Torr, which is described in detail elsewhere.³⁴ The onset and cessation of growth was detected by in situ spectroscopic ellipsometry at an incident angle (relative to the surface normal) of 70°, and the ellipsometric parameter Psi was measured at several wavelengths. The wavelength for data collection was chosen so that changes in Psi due to growth are easily observed; this wavelength varies by substrate, temperature, and deposited material. Before aligning the ellipsometer and introducing the precursor, substrates were maintained at the deposition temperature for at least 15 min to allow the substrate temperature to stabilize. To test for area selective growth, experiments were performed using parallel dosing on Au and Al₂O₃ substrates; growth was allowed us to proceed 4 min after the onset of nucleation on Au, as detected by ellipsometry. Area selective growth was also probed in single experiments for the $\mathrm{Hf}(\mathrm{BH_4})_4\text{-}\mathrm{TMAA}$ system by comparing the nucleation delay on an oxide substrate, Si native oxide, against the nucleation delay on a metal substrate formed by brief deposition of Al and subsequent flow from Hf(BH₄)₄ alone.

Static CVD experiments, where static refers to the absence of dynamic pumping, were conducted in a chamber consisting of a Pyrex glass tube that was closed at one end and fitted with a vacuum flange at the other end. The vacuum flange was connected to a turbomolecular pump through a gate valve and to the precursor reservoirs by stainless steel precursor delivery lines equipped with shut-off valves.³⁵ A capacitance manometer monitored the total chamber pressure.

Growth under static CVD conditions was carried out by placing the glass tube loaded with substrates in a tube furnace and baking them for 2 h at 250 °C under a dynamic vacuum. The tube was then cooled to room temperature, isolated from the turbopump, and charged with precursors to total pressures on the order of 1 Torr. The temperature of the tube furnace and chamber was then ramped from room temperature while monitoring the pressure. Gas heating during the temperature ramp causes the total pressure to increase (Gay-Lussac's law), but this increase is gradual and easily distinguished from the pressure increase due to the onset of deposition.

Compositional depth profiling of the resulting films was performed by Rutherford backscattering spectrometry (RBS, NEC Pelletron accelerator) and time-of-flight secondary ion mass spectroscopy (SIMS, PHI Trift III). RBS data were fit to layered compositional profiles using SIMNRA software; the fit error for Hf is estimated by the software to be <1.5%. For growth on two surfaces, the selectivity factor is $Selectivity = \frac{\theta_G - \theta_{NG}}{\theta_G + \theta_{NG}},$ where θ is the amount deposited on growth (G) and nongrowth (NG) surfaces. The amount of HfB₂ deposited from Hf(BH₄)₄ was calculated from the areal density of Hf deposited on each substrate, $\frac{1}{2}\frac{1}{8}\frac{1$ Pelletron accelerator) and time-of-flight secondary ion mass spec-

Selectivity =
$$\frac{\theta_G - \theta_{NG}}{\theta_G + \theta_{NG}}$$

calculated from the areal density of Hf deposited on each substrate, $\frac{\omega}{2}$ as measured by RBS. In cases where aluminum nucleation was not uniform, and growth instead proceeded to form nanocrystals, scanning electron microscopy (SEM, Hitachi S4800) was used to determine the presence or absence of nuclei. X-ray diffraction patterns were measured on a Bruker D8 Advance instrument.

III. RESULTS AND DISCUSSION

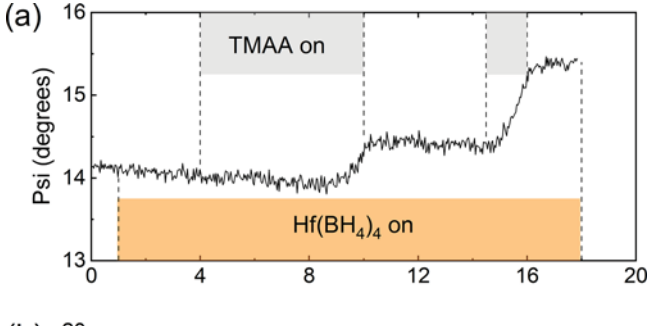
A. Deposition of aluminum from TMAA is inhibited by Hf(BH₄)₄

The first pair of precursors we investigated, TMAA/Hf(BH₄)₄, is of interest in the context of the growth of $Hf_{1-x}Al_xB_v$ alloys for



application as oxidation-resistant protective coatings.³⁶ These two precursors have different reaction onset temperatures ($T_{\rm g}$) when used individually: 130 °C for TMAA but 170 °C for Hf(BH₄)₄. It was anticipated that, when both precursors are passed simultaneously over a heated substrate, the film would consist almost entirely of aluminum between 130 and 170 °C, but would contain increasing amounts of hafnium and boron above 170 °C. This is not what happens.

When Si/SiO_2 substrates at 150 °C are exposed to TMAA alone, nucleation is hard to detect by ellipsometry, but the formation of isolated crystals occurs more or less instantaneously (<1 min), as observed by *ex situ* SEM (see Fig. S1 in the supplemental material). As expected, if the Si/SiO_2 substrates at 150 °C are exposed to 0.22 mTorr of $Hf(BH_4)_4$ alone, no HfB_2 deposition occurs because the surface is below the onset temperature for growth from this precursor. If this latter experiment is continued by adding 0.005 mTorr of TMAA to the flow, no growth is detected by ellipsometry until *after* a 4 min nucleation delay [Fig. 1(a)]. Thus, $Hf(BH_4)_4$ inhibits nucleation from TMAA at this temperature. After nucleation starts, growth then continues as long as TMAA is present, but stops immediately if TMAA flow is discontinued and only $Hf(BH_4)_4$ is passed over the substrates; this result confirms that the growth is due to the deposition of aluminum.



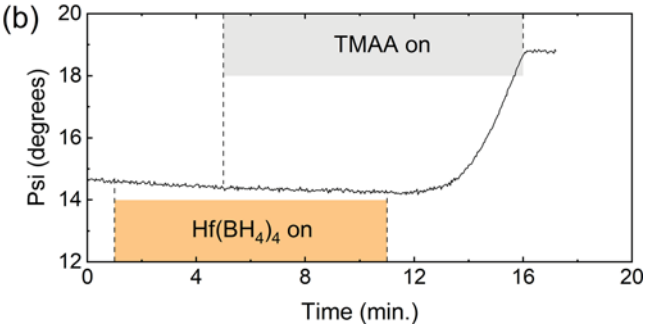


FIG. 1. Ellipsometry parameter Psi (λ = 427.2 nm) during Hf(BH₄)₄ and TMAA injection at 150 °C in continuously pumped CVD on Si covered with native oxide: Hf(BH₄)₄ delays TMAA nucleation, but it does not suppress growth. Increasing the Hf(BH₄)₄ flux extends the nucleation delay. Results using 0.220 and 0.320 mTorr Hf(BH₄)₄ are shown in (a) and (b), respectively. In (b), growth from TMAA begins soon after the Hf(BH₄)₄ flow is terminated. From the film shown in (b), *ex situ* RBS shows a small amount of Hf present on the interface between the substrate and the Al film (Fig. S2 in the supplemental material⁵¹).

At this point, 4 min after continuing to pass $Hf(BH_4)_4$ over the substrates with no further growth being detected, TMAA was readded to the flow. Film growth resumes almost immediately without a noticeable delay. This finding shows that, whereas $Hf(BH_4)_4$ inhibits nucleation on the bare Si/SiO_2 substrate, it does not inhibit growth on already-formed aluminum nuclei and islands. This behavior is desirable for ASD: nucleation is inhibited on one substrate, Si with native oxide, whereas growth proceeds on the freshly deposited aluminum.

If the inhibition is due to competitive adsorption between the two precursors, then increasing the Hf(BH₄)₄ (inhibitor) pressure should lengthen the nucleation delay from TMAA. For an experiment identical to that above, except that the Hf(BH₄)₄ pressure was 0.32 instead of 0.22 mTorr, the ellipsometry data indicate such a dependence [Fig. 1(b)]: the nucleation delay during coflow increases to at least 6 min instead of 4. If the Hf(BH₄)₄ pressure is reduced to 0.10 mTorr, the nucleation delay is only 1.5 min [data resemble those in Fig. 1(a) with inflection due to growth at the 5.5 min mark]. When the 0.320 mTorr Hf(BH₄)₄ coflow is shut off after the initial 6 min, aluminum begins to grow immediately. This experiment shows that the nucleation delay for Al growth from TMAA lengthens with increasing Hf(BH₄)₄ pressure, and passivation of the Si/SiO₂ surface toward Al deposition requires a continuous flow of Hf(BH₄)₄.

It is worth noting that the nucleation of aluminum is not intrinsically uniform on SiO₂–Si substrates so that the onset of nucleation from TMAA alone is difficult to detect by ellipsometry because Al is in the form of disperse islands instead of continuous films. During or after Hf(BH₄)₄ coflow, however, the onset of Al growth is easily detectable by ellipsometry, which can be associated with the onset of uniform film growth instead of sparse growth on isolated defects. Therefore, the effect of Hf(BH₄)₄ on Al nucleation is nuanced: Hf(BH₄)₄ increases the areal density of nucleation sites on the substrates, but, at an increasing Hf(BH₄)₄ pressure, competitive adsorption prevents this nucleation from occurring. Plan-view SEM images of the films grown in this study indicate this transition from defect-dependent nucleation without Hf(BH₄)₄ flux to dense nucleation at low Hf(BH₄)₄ flux to comparably sparse, but uniformly distributed, nucleation at high Hf(BH₄)₄ flux (see Fig. S1 in the supplemental material).⁵¹

Static CVD conditions, using higher (Torr) pressures, show similar behavior. The nonpumped borosilicate glass chamber was charged at room temperature with 2 Torr of Hf(BH₄)₄ and 0.5 Torr of TMAA, either individually or combined. Deposition was monitored from pressure versus time during the temperature ramp (Fig. 2): the deposition of Al from one mole of TMAA yields 2.5 moles of gas (one equivalent of NMe₃ and 1.5 equivalents of H₂), and the deposition of HfB₂ from one mole of Hf(BH₄)₄ ideally yields 6 moles of gas (one equivalent of B₂H₆ and five equivalents of H₂). These data show that, as expected, the onset of TMAA deposition occurs at 130 °C and the onset of Hf(BH₄)₄ deposition occurs at 170 °C when these precursors are used individually.

In contrast, with combined precursors, no pressure rise corresponding to the TMAA reaction occurs between 130 and 170 °C, which takes place over 20 min of temperature ramping; the pressure begins to rise due to deposition only at 170 °C. An identical experiment, using the same pressure and temperature

ramp conditions, confirms the inhibition by $Hf(BH_4)_4$ in this temperature window. At a constant temperature of 150 °C [i.e., a temperature at which the deposition of TMAA is inhibited by a coflow of $Hf(BH_4)_4$], sequential dosing of $Hf(BH_4)_4$ (and subsequent pump-out) TMAA shows no sign of inhibition (see Fig. S3 in the supplemental material).⁵¹

Thus, at temperatures between 130 and 170 °C, Al growth from TMAA on Si/SiO₂ is inhibited only when Hf(BH₄)₄ flux is simultaneously present. This result suggests that the Hf(BH₄)₄ inhibitor populates Si/SiO₂ surface sites dynamically, e.g., as described by a Langmuir isotherm for surface coverage.³⁷ The small amount of Hf present on the surfaces after these experiments suggests that at least some Hf(BH₄)₄ chemisorption is present in this system (see Fig. S2 in the supplemental material).⁵¹ The inhibition probably occurs by site-blocking; this hypothesis is consistent with the reported mechanism for Al deposition from TMAA, which requires two sites, one for initial precursor adsorption and the other for removal of the NMe₃ ligand.³¹ Coadsorption of Hf(BH₄)₄ reduces the availability of primary adsorption sites and the nearby second sites necessary for TMAA to react.

The site-blocking mechanism on the uncoated substrate is supported by the composition of the resulting films after the continued temperature ramp beyond 170 °C, above which HfB₂ deposition is expected to occur simultaneously with Al, during growth under static CVD conditions. For a film whose growth was stopped before the depletion of either precursor, the average film

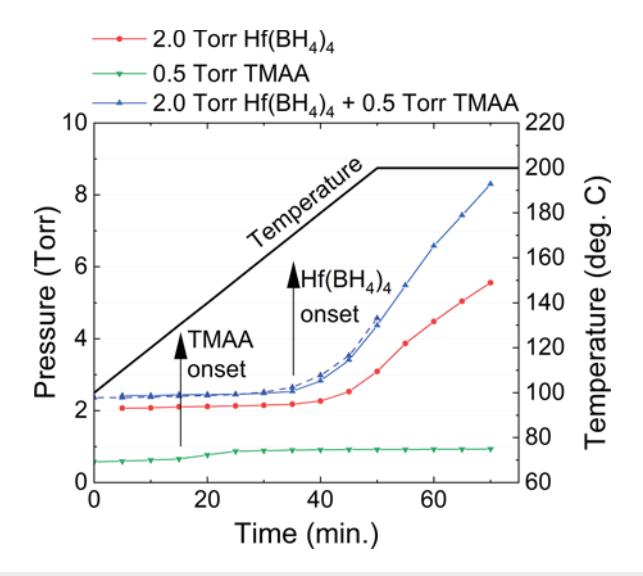
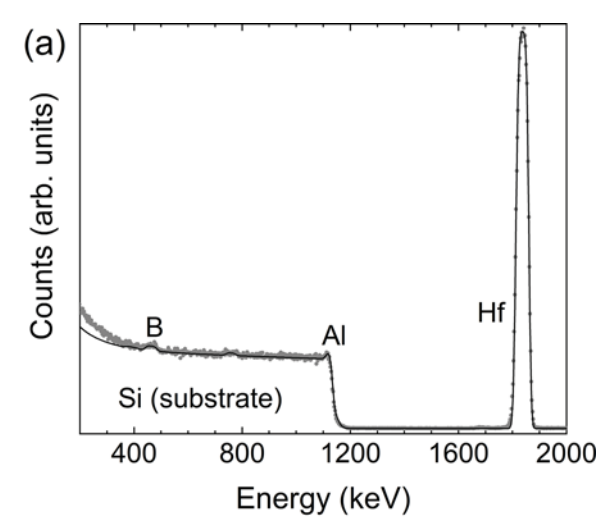


FIG. 2. Total pressure (connected points) recorded during deposition from $Hf(BH_4)_4$ and/or TMAA in the static CVD reactor. The green and red curves and the black arrows indicate the growth onset temperature for each precursor used alone. The blue curves indicate that, when both precursors are present, no pressure increase occurs until the onset temperature for $Hf(BH_4)_4$; for the blue dashed curve, growth was stopped at the end of the temperature ramp, whereas in the solid blue curve, growth was continued until complete precursor consumption (beyond the time marked on the graph). Both results had identical growth onset temperatures within an experimental error of 170 °C.

composition measured by RBS is $Hf_{0.65}Al_{0.35}B_2$ [Fig. 3(a)]. SIMS depth profiling [Fig. 3(b)] shows that there is a gradient in Al content: It is the highest near the Si substrate (i.e., at early times) and lower nearer the top surface of the films (i.e., later times). This result is consistent with the site-blocking mechanism because (1) $Hf(BH_4)_4$ does not inhibit Al deposition after the



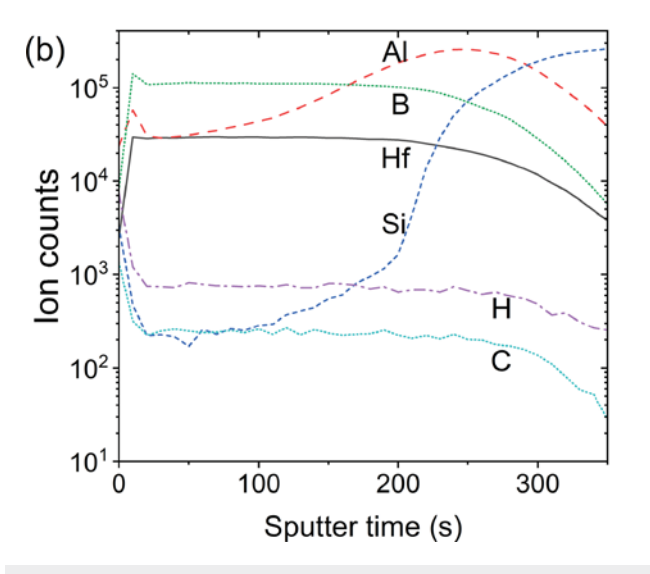


FIG. 3. Compositional depth profiles for the alloy film, grown from 2 Torr Hf(BH₄)₄ and 0.5 Torr TMAA. Growth of this sample was stopped at the end of the temperature ramp to 200 °C (dashed curve in Fig. 2). (a) RBS and (b) SIMS analyses indicate the average composition and compositional gradients, respectively. RBS measures 786.5 Hf atoms nm $^{-2}$ and 430 Al atoms nm $^{-2}$. SIMS indicates a small increase in C content in the film relative to the substrate. N ion counts (not shown) are low ($\sim \! 10^1\!)$ and constant across the film and substrate regions, indicating no N contribution from film growth. AlH $^+$ ions interfere with the calculation of Si counts from SIMS data, causing the initial trend in Al composition to be reflected in the number of Si counts; the strong change in slope indicates that the substrate is reached after 200 s of sputtering.

onset of nucleation, (2) the reaction probability of TMAA at these temperatures is higher than that for Hf(BH₄)₄, ³⁶ which leads to a faster depletion in TMAA pressure relative to Hf(BH₄)₄, and (3) the gas phase pressure of TMAA under these static CVD conditions falls with time. Furthermore, the x-ray diffraction pattern (see Fig. S4 in the supplemental material)⁵¹ shows that the film contains no embedded face-centered cubic Al nuclei but, instead, is an essentially amorphous alloy. Compositionally uniform films can be obtained at temperatures over 170 °C in pumped CVD conditions at constant precursor fluxes,³⁶ with the trade-off that the precursor utilization efficiency is low. All of the precursors that exit in the deposition zone are discarded via pump exhaust.

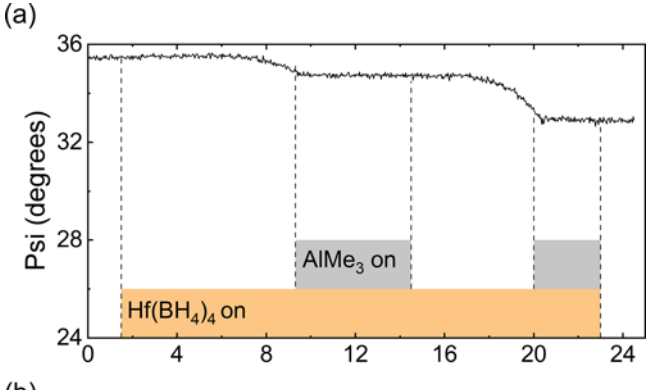
Metal borohydride compounds have not previously been reported as surface passivating agents in film deposition experiments, so these results establish a new surface termination, i.e., borohydride, that should be considered for passivating reactive sites. The nearest analogous phenomena are the formation of self-assembled monolayers from decaborane thiols, in which the thiols bind to the substrate to form a decaborane-terminated surface, ¹⁰ and of boranes to poison catalytic surfaces. ^{38,39}

B. Deposition of HfB₂ from Hf(BH₄)₄ is inhibited by AIMe₃

The second pair of precursors, AlMe₃/Hf(BH₄)₄, was explored to determine whether AlMe₃—a more readily available precursor—could replace TMAA as an aluminum source for the growth of Hf_{1-x}Al_xB_y alloys. One consequence of this change is that the onset temperatures of the Al and Hf precursors are reversed: $T_{\rm g} = 300~{\rm ^{\circ}C}$ for AlMe₃, which, unlike TMAA at 130 °C, is *higher* than that for Hf(BH₄)₄. Initial experiments are performed at 250 and 275 °C, where growth is expected from Hf(BH₄)₄, and no growth is expected from AlMe₃.

In the flow CVD system at 250 °C, 0.12 mTorr of Hf(BH₄)₄ is passed over an SiN_x substrate until HfB₂ nucleation is detected via ellipsometry (the parameter Psi begins to decrease over time), and then, 0.10 mTorr AlMe₃ is coflowed. When AlMe₃ is introduced into the system, the ellipsometry parameter Psi stops changing with time, indicating the cessation of HfB₂ growth that correlates with the introduction of AlMe₃ [Fig. 4(a)]. After about 5 min of coflow without growth, the AlMe₃ source is shut off. Interestingly, HfB₂ growth resumes, but only after a 3-min delay. This result suggests that the inhibitory effect of AlMe₃ on the surface persists for short times but is eventually reversible, potentially by desorption or by reaction with vacuum contaminants, such as moisture from the chamber walls.

A similar experiment tested inhibition at a higher substrate temperature of 275 °C and a smaller ratio of AlMe₃ to Hf(BH₄)₄ pressures (1:10 versus \sim 1:1 in the experiment above). As in the experiment above, HfB₂ growth is initiated from 0.20 mTorr of Hf(BH₄)₄ before introducing 0.02 mTorr of AlMe₃ coflow. During coflow, the growth of HfB₂ decreases to a small but nonzero rate, indicating a limit to the ability of AlMe₃ to inhibit HfB₂ growth close to the former's growth onset temperature [Fig. 4(b)]. The ellipsometry data indicate that the HfB₂ growth rate decreases by \sim 35× during AlMe₃ coflow; note that the film is not continuous



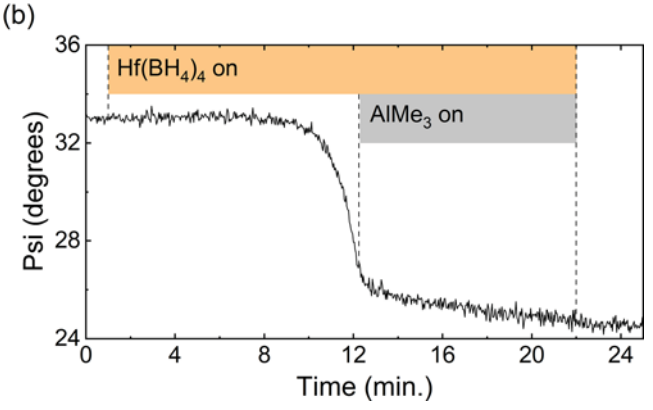


FIG. 4. In situ ellipsometry parameter Psi (λ = 601.2 nm) shows the onset, propagation, and cessation of HfB₂ growth during screening experiments on SiN_x substrates for (a) 0.10 mTorr AlMe₃ inhibition of 0.12 mTorr Hf(BH₄)₄ at 250 °C and (b) 0.02 mTorr AlMe₃ inhibition of 0.21 mTorr Hf(BH₄)₄ at 275 °C.

(SEM images in Fig. S5 in the supplemental material), 51 so the relative growth rate is imprecise.

The persistence of inhibition by AlMe₃ contrasts with the immediate resumption of growth observed in the TMAA/Hf(BH₄)₄ system when the inhibitor flow is stopped. In other words, IHf(BH₄)₄ exerts its inhibitory influence only while it is present in the gas flux, whereas AlMe₃ continues to inhibit growth for some time even after its flux to the substrate ceases. Evidently, the surface quickly returns to the noninhibited state for nonpersistent pinhibitors, but the surface is changed in such a way that the return to the noninhibited state is slow for longer-lasting inhibitors. It remains unknown how AlMe₃ adsorbs to the HfB₂ nuclei grown on the SiN_x substrates; a future investigation with *in situ* chemical analysis may provide a good comparison with AlMe₃ adsorption on the other surfaces.

The persistent inhibitory effect of AlMe₃ is not entirely surprising because methyl groups are known to provide surface passivation for area selective deposition, ¹ and AlMe₃ is known to convert hydroxylated surfaces to methyl- (i.e., methoxy-) terminated surfaces below its growth temperature. ^{40–43} On the other hand, AlMe₃ does not adsorb as densely on nonhydroxylated surfaces. This

TABLE I. Hf incorporation (atoms nm⁻²) after 4 min growth of HfB₂ from Hf(BH₄)₄, as measured by RBS.

Substrate	No predosing	Predosed with AlMe ₃ for 6 min
Al ₂ O ₃ on Si	7.2	0.8
Au on SiO ₂	337.5	288
Selectivity factor	0.958	0.994

difference suggests that AlMe3 may enable selective growth on metallic or dehydroxylated surfaces, while no growth occurs on hydroxylated surfaces. The following experiments explore the use of AlMe₃ to selectively inhibit the onset of HfB₂ growth as a function of the substrate composition, oxide versus metal. Note that AlMe3 will stop the growth of HfB2 after it has nucleated, as observed in the initial experiments: so AlMe₃ inhibition is applied as a pretreatment rather than as a continuous flow.

To test this suggestion, we examined the growth of HfB2 from 0.12 mTorr Hf(BH₄)₄ on Au versus Al₂O₃ at 250 °C with and without 6 min of predosing the surface with 0.10 mTorr of AlMe₃. After 4 min of growth, the areal density of Hf (in HfB2) was measured by RBS on all four substrates (Table I; spectra in Fig. S6 in the supplemental material).⁵¹ We calculated the selectivity factor from these quantities.⁵ Although some of the difference between growth on the two substrates can be attributed to intrinsic selectivity (i.e., HfB2 more readily nucleates on metallic surfaces than on oxides),³⁰ AlMe₃ coflow increases the selectivity from 95.8% (intrinsic) to 99.4% (with AlMe₃ pretreatment). This increased selectivity has a major practical importance because it increases the thickness that can be grown before etching back unwanted nuclei

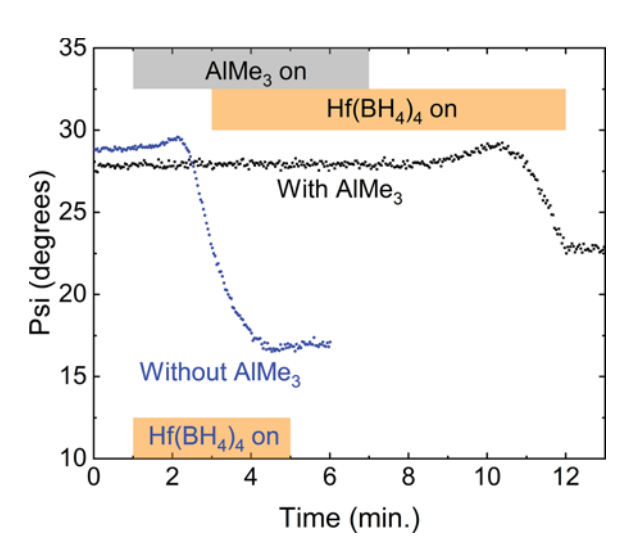


FIG. 5. *In situ* ellipsometry parameter Psi (λ = 594.7 nm) vs time for deposition from Hf(BH₄)₄ on an Au substrate in the presence of AlMe₃ (black, points shown for 0-13 min) or absence of AlMe₃ (blue, points shown for 0-6 min) at 250 °C from 0.12 mTorr Hf(BH₄)₄ and 0.10 mTorr AlMe₃. Precursor flow times are indicated on the graph.

becomes necessary. 44,45 For ASD of thicker HfB2 films, it might be possible to renew the inhibition on Al₂O₃ using pulsed or low pressure AlMe3 rather than by adding an etch-back step. Overall, this experiment serves as a proof-of-concept for selective surface passivation by AlMe₃.

On Au, HfB2 deposition begins quickly when the surfaces are not exposed to AlMe₃ before or during Hf(BH₄)₄ (Fig. 5). In contrast, no HfB2 film nucleation is observed on Au during the coflow of the two precursors. After the AlMe₃ flow is stopped but the flow of Hf(BH₄)₄ is continued, it takes about a minute for HfB₂ growth to resume, and less Hf was deposited compared to the control experiment with no AlMe₃ coflow (Table I).

C. Deposition of aluminum from TMAA is inhibited by AlMe_z

The results above suggest that AlMe₃ may also be able to block the growth of Al from TMAA at temperatures between 130° C (T_g for TMAA) and 300 °C (T_g for AlMe₃). Si/SiO₂ substrates were treated with 0.03 mTorr of AlMe₃ for 2 min at 200 °C and then 0.02 mTorr of TMAA was added to the flux. No growth is detected during the periods of coflow, but the onset of Al film C (T_g for TMAA) and 300 °C (T_g for AlMe₃). Si/SiO₂ substrates growth commences about 2-3 min after AlMe₃ flow is stopped $\frac{\omega}{\underline{\underline{\omega}}}$ while TMAA flow continued (Fig. 6).

Plan-view SEM of the two samples grown in these experiments confirms the inhibition effect. Substrates exposed to a continuous coflow of 0.03 mTorr of AlMe₃ and 0.02 mTorr of TMAA for 13 min show no sign of Al nucleation [Fig. 7(a)]. In contrast, octahedral Al nuclei are distributed across the surface of substrates

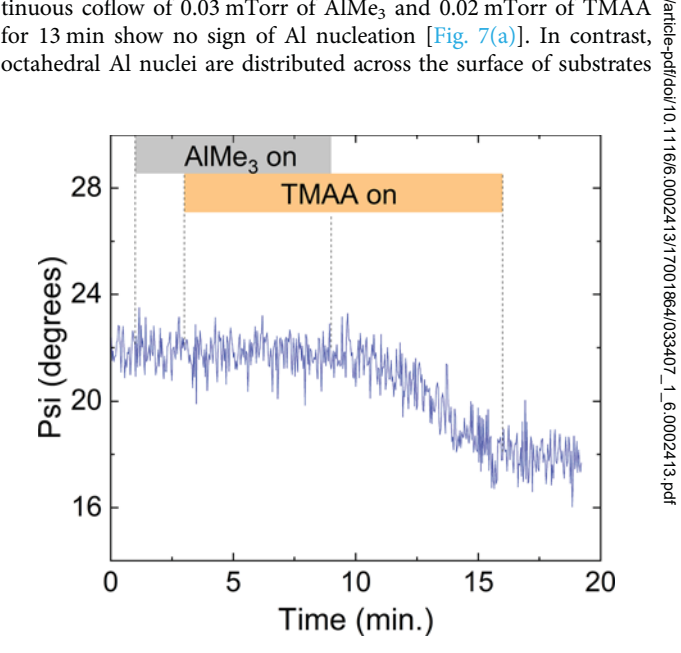
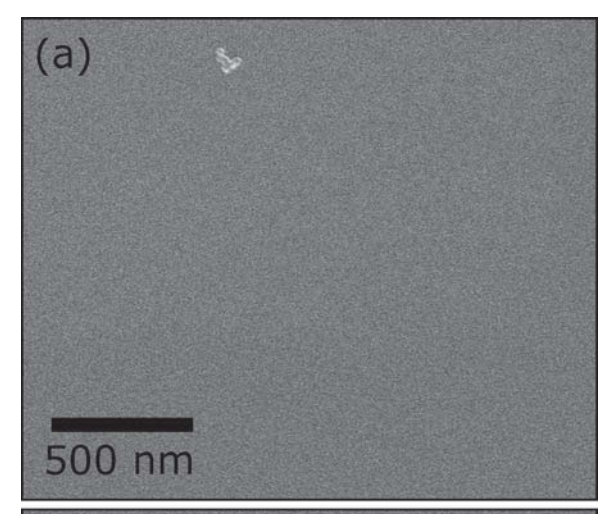


FIG. 6. In situ ellipsometry parameter Psi (λ = 339 nm) shows the onset of nucleation and growth from TMAA after stopping AlMe₃ coflow on Si/SiO₂ substrates at 200 °C. Precursor pressures are 0.03 mTorr for AIMe₃ and 0.02 mTorr for TMAA. In a comparison experiment with AlMe3 coflow during the entire 13-min period of TMAA flow, ellipsometry data (see Fig. S7 in the supplemental material⁵¹) indicate no growth.

exposed to a coflow of AlMe₃ and TMAA at the same pressures for the first 6 min, then a flow of TMAA alone for 7 min [Fig. 7(b)].

One distinction between this result and the inhibition by $Hf(BH_4)_4$ is the duration of the passivation effect: $Hf(BH_4)_4$ inhibition of Al nucleation from TMAA ends immediately after the flow of the inhibitor is stopped, whereas AlMe₃ inhibition of HfB_2 growth from $Hf(BH_4)_4$, as well as Al growth from TMAA, persists even after the flow of the inhibitor ends. These experiments show that $AlMe_3$ can inhibit growth from CVD precursors of very different types. Another distinction between these systems is whether the inhibitor affects only nucleation, only growth, or both. $Hf(BH_4)_4$ inhibits the nucleation of aluminum from TMAA, but it does not



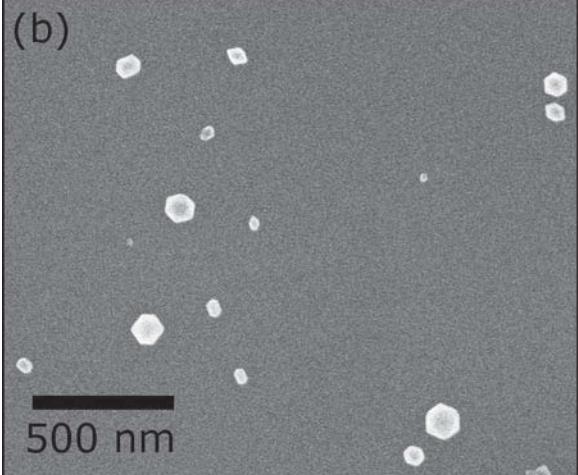


FIG. 7. Plan-view SEM shows the presence or absence of Al nuclei on Si substrates with native oxide after testing AIMe₃ inhibition of TMAA nucleation at 200 °C: (a) film exposed to a continuous coflow of AIMe₃ and TMAA and (b) film exposed to a coflow of AIMe₃ and TMAA for the first 6 min, then flow of TMAA alone for 7 min. Precursor pressures are 0.03 mTorr for AIMe₃ and 0.02 mTorr for TMAA. The image in (a) includes a piece of debris used to focus on the surface.

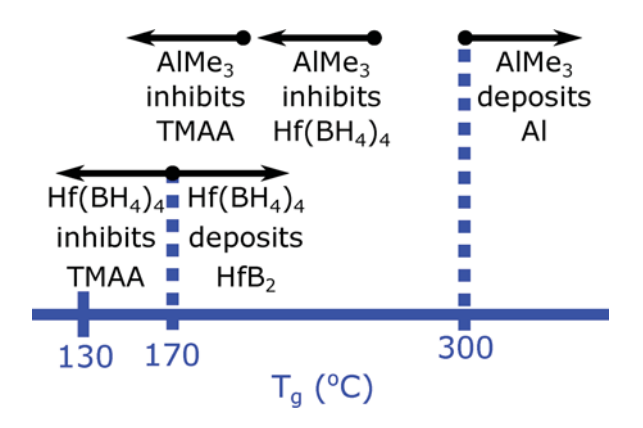


FIG. 8. Temperature ranges for nucleation or growth inhibition as a function of $T_{\rm g}$ for the precursors described: TMAA ($T_{\rm g}$ = 130 °C), Hf(BH₄)₄ ($T_{\rm g}$ = 170 °C), and AlMe₃ ($T_{\rm g}$ = 300 °C).

prevent steady-state growth of Al on the surfaces where Al growth has already occurred. In contrast, AlMe₃ inhibits the nucleation and growth of HfB_2 from $Hf(BH_4)_4$.

IV. CONCLUSIONS

We show that area selective chemical vapor deposition can be enhanced using a pair of CVD precursors that have different growth onset temperatures. When growth is conducted at a temperature between the onset temperatures, one precursor that would normally react to afford film may have its nucleation or growth inhibited by a second precursor that has a higher growth onset temperature (Fig. 8).

In both systems in which ASD is observed, Hf(BH₄)₄-TMAA and AlMe₃-Hf(BH₄)₄, the inhibitor enhances the preference to grow selectively on metal substrates over oxides. The evidence for the former is produced by continued growth on the existing Al nuclei instead of the surrounding silica surfaces, and the latter is shown by a parallel precursor dosing on the Au and Al₂O₃ substrates. Although we have not carried out any mechanistic studies to determine exactly how the inhibitors enhance ASD, the known surface chemistry of these precursors immediately suggests possible causes. For example, AlMe₃ nucleates densely on oxides to form methyl-terminated surfaces, which resemble other passivated surfaces in ASD, whereas AlMe₃ nucleates sparsely on metals. 42,43,46 Similarly, the borohydride groups in Hf(BH₄)₄ can react with surface hydroxyl groups to form B–O bonds, ^{16,47} a reaction that is likely to lengthen the surface residence time of the precursor and its reaction products on oxides but not on metals. ⁷

These results suggest that there is much room to identify new molecules to use as selective CVD and ALD inhibitors and to enhance ASD. In general, potential growth inhibitors that may be useful for ASD are those that chemisorb very differently between surfaces that contain versus lack surface hydroxyl groups. ^{48–50} ALD precursors, such as AlMe₃, appear to be particularly well suited to serve as growth inhibitors from other precursors. The self-limiting coverage of the ALD precursors implies that the molecules



passivate the surface toward themselves, and, thus, they may also render the surface inert toward other precursor molecules.

Follow-up studies may explore these other paths for ASD using inhibitors that are also used as precursors for film growth, and they may also probe the chemical details of the surfaces involved. For the $Hf(BH_4)_4$ -AlMe3 system, for example, measurements may probe chemical functional groups on the starting substrate, on the HfB_2 film as growth proceeds, and on the film after AlMe3 have been introduced to make the surface no longer reactive. The effect of $Hf(BH_4)_4$ on Al nucleation from TMAA may also support future work to discern which mechanism governs nucleation enhancement at low $Hf(BH_4)_4$ pressures and inhibition at high $Hf(BH_4)_4$ pressures.

ACKNOWLEDGMENTS

The authors thank Robert J. Lastowski and Christopher M. Caroff for preparing the Hf(BH₄)₄ precursor used in these experiments and loading the air-sensitive precursors into sample vessels. This work was funded by NSF (No. CMMI 18-25938) (to J.R.A.) and by NSF (Grant No. CHE 19-54745) (to G.S.G.). Materials characterization was carried out in part at the Materials Research Laboratory Central Research Facilities, University of Illinois.

AUTHOR DECLARATIONS

Conflict of Interest

The authors have no conflicts to disclose.

Author Contributions

Kinsey L. Canova: Conceptualization (equal); Formal analysis (equal); Investigation (equal); Writing – original draft (equal); Writing – review & editing (equal). Laurent Souqui: Validation (equal); Writing – review & editing (equal). Gregory S. Girolami: Methodology (equal); Validation (equal); Writing – review & editing (equal). John R. Abelson: Conceptualization (supporting); Funding acquisition (equal); Supervision (equal); Validation (equal); Writing – review & editing (equal).

DATA AVAILABILITY

The data that support the findings of this study are available within the article and its supplementary material.

REFERENCES

- ¹J. Yarbrough, A. B. Shearer, and S. F. Bent, J. Vac. Sci. Technol. A **39**, 021002 (2021).
- ²G. N. Parsons and R. D. Clark, Chem. Mater. 32, 4920 (2020).
- ³G. N. Parsons, J. Vac. Sci. Technol. A 37, 020911 (2019).
- ⁴C. Nender, I. V. Karardjiev, A. M. Barklund, S. Berg, and P. Carlsson, Thin Solid Films **228**, 87 (1993).
- ⁵W. L. Gladfelter, Chem. Mater. 5, 1372 (1993).
- ⁶Y. J. Lee and S.-W. Kang, Electrochem. Solid State Lett. 5, C91 (2002).
- ⁷D. Choudhury et al., J. Vac. Sci. Technol. A 38, 042407 (2020).
- ⁸D. Bobb-Semple, K. L. Nardi, N. Draeger, D. M. Hausmann, and S. F. Bent, Chem. Mater. **31**, 1635 (2019).

- ⁹F. S. M. Hashemi, C. Prasittichai, and S. F. Bent, J. Phys. Chem. C 118, 10957 (2014).
- ¹⁰J. Bould, J. Machacek, M. G. S. Londesborough, R. Macias, J. D. Kennedy, Z. Bastl, P. Rupper, and T. Base, <u>Inorg. Chem.</u> 51, 1685 (2012).
- ¹¹N. L. Jeon, W. Lin, M. K. Erhardt, G. S. Girolami, and R. G. Nuzzo, Langmuir 13, 3833 (1997).
- ¹²M. J. M. Merkx, T. E. Sandoval, D. M. Hausmann, W. M. M. Kessels, and A. J. M. Mackus, Chem. Mater. **32**, 3335 (2020).
- ¹³T. K. Talukdar, G. S. Girolami, and J. R. Abelson, J. Vac. Sci. Technol. A 37, 021509 (2019).
- 14 A. Yanguas-Gil, J. A. Libera, and J. W. Elam, Chem. Mater. 25, 4849 (2013).
- ¹⁵E. Mohimi, Z. V. Zhang, S. Liu, J. L. Mallek, G. S. Girolami, and J. R. Abelson, J. Vac. Sci. Technol. A 36, 041507 (2018).
- ¹⁶Z. V. Zhang, S. Liu, G. S. Girolami, and J. R. Abelson, J. Vac. Sci. Technol. A 39, 023415 (2021).
- 17R. Khan et al., Chem. Mater. 30, 7603 (2018).
- ¹⁸J. Soethoudt, Y. Tomczak, B. Meynaerts, B. T. Chan, and A. Delabie, J. Phys. Chem. C 124, 7163 (2020).
- 19J. Soethoudt, S. Crahaij, T. Conard, and A. Delabie, J. Mater. Chem. C 7, § 11911 (2019).
- 20 Z. Xue, H. Thridandam, H. D. Kaesz, and R. F. Hicks, Chem. Mater. 4, 162 (1992).
- ²¹D. P. Adams, L. L. Tedder, T. M. Mayer, B. S. Swartzentruber, and E. Chason, Phys. Rev. Lett. **74**, 5088 (1995).
- ²²M. Hiratani, T. Nabatame, Y. Matsui, K. Imagawa, and S. Kimura, J. Electrochem. Soc. **148**, C524 (2001).
- ²³W. L. Gladfelter, D. C. Boyd, and K. F. Jensen, Chem. Mater. 1, 339 (1989).
- ²⁴M. J. Cooke, R. A. Heinecke, R. C. Stern, and J. W. Maes, Solid State Technol. 25, 62 (1982).
- ²⁵R. Phillips and E. Eisenbraun, ECS Trans. 35, 27 (2011).
- ²⁶L.-Y. Chen, M. Naik, T. Guo, and R. C. Mosely, U.S. patent 6,139,905 (11 April 1997).
- ²⁷C. T. Nguyen *et al.*, Nat. Commun. **13**, 7597 (2022).
- ²⁸D. B. Beach, S. E. Blum, and F. K. LeGoues, J. Vac. Sci. Technol. A 7, 3117 (1989)
- ²⁹S. Jayaraman, Y. Yang, D. Y. Kim, G. S. Girolami, and J. R. Abelson, J. Vac. Sci. Technol. A 23, 1619 (2005).
- ³⁰Y. Yang, S. Jayaraman, D. Y. Kim, G. S. Girolami, and J. R. Abelson, Chem. Mater. 18, 5088 (2006).
- 31T. T. Kodas and M. J. Hampden-Smith, *The Chemistry of Metal CVD* (VCH Inc., New York, 1994).
- ³²A. L. Wayda, L. F. Schneemeyer, and R. L. Opila, Appl. Phys. Lett. **53**, 361 (1988).
- ³³K. B. Borisenko, A. J. Downs, H. E. Robertson, D. W. H. Rankin, and C. Y. Tang, Dalton Trans. **2004**, 967 (2004).
- ³⁴K. L. Canova, Z. V. Zhang, G. S. Girolami, and J. R. Abelson, J. Vac. Sci. Technol. A 39, 013402 (2021).
- 35 A. N. Cloud, "Ultraconformal chemical vapor deposition and synthesis of transition metal nitride films," Ph.D. thesis (University of Illinois at Urbana-Champaign, 2013).
- ³⁶K. L. Canova, "Growth kinetics and microstructure in two precursor chemical vapor deposition of borides," Ph.D. thesis (University of Illinois Urbana-Champaign, 2022).
- ³⁷C. J. Taylor, D. C. Gilmer, D. G. Colombo, G. D. Wilk, S. A. Campbell, J. Roberts, and W. L. Gladfelter, J. Am. Chem. Soc. 121, 5220 (1999).
- ³⁸C. A. Jaska, T. J. Clark, S. B. Clendenning, D. Grozea, A. Turak, Z.-H. Lu, and I. Manners, J. Am. Chem. Soc. 127, 5116 (2005).
- ³⁹M. Söderlund, P. Mäki-Arvela, K. Eränen, T. Salmi, R. Rahkola, and D. Y. Murzin, Catal. Lett. 105, 191 (2005).
- ⁴⁰P. Boryło, K. Lukaszkowicz, M. Szindler, J. Kubacki, K. Balin, M. Basiaga, and J. Szewczenko, Vacuum 131, 319 (2016).
- ⁴¹M. Juppo, A. Rahtu, M. Ritala, and M. Leskelä, <u>Langmuir</u> 16, 4034 (2000).

- 47S. Babar, N. Kumar, P. Zhang, J. R. Abelson, A. C. Dunbar, S. R. Daly, and G. S. Girolami, Chem. Mater. **25**, 662 (2013).

 48J.-S. Kim and G. N. Parsons, Chem. Mater. **33**, 9221 (2021).
- 49H. Saare, S. K. Song, J.-S. Kim, and G. N. Parsons, J. Appl. Phys. 128, 105302
- 50G. N. Parsons, B. Kalanyan, S. E. Atanasov, P. Lemaire, and C. Oldham, ECS Trans. 75, 77 (2016).
- 51 See the supplementary material at https://www.scitation.org/doi/suppl/ 10.1116/6.0002413 for supporting materials referred to in the main text.

⁴²J. S. Lee, T. Kaufman-Osborn, W. Melitz, S. Lee, A. Delabie, S. Sioncke, M. Caymax, G. Pourtois, and A. C. Kummel, J. Chem. Phys. 135, 054705 (2011).

43 Z. Gao, "Nucleation and growth of atomic layer deposition: Effect of substrate

and precursor chemistry," Ph.D. thesis (Washington University, 2018).

⁴⁴ M. Bonvalot, C. Vallee, C. Mannequin, M. Jaffal, R. Gassilloud, N. Posseme, and T. Chevolleau, Dalton Trans. 51, 442 (2022).

45 M. F. J. Vos, S. N. Chopra, M. A. Verheijen, J. G. Ekerdt, S. Agarwal,

W. M. M. Kessels, and A. J. M. Mackus, Chem. Mater. 31, 3878 (2019).

⁴⁶B. R. Rogers, Thin Solid Films 408, 87 (2002).